Journal of Organometallic Chemistry 695 (2010) 546–551

Contents lists available at ScienceDirect

Journal of Organometallic Chemistry

journal homepage: www.elsevier.com/locate/jorganchem

Triorganotin(IV) derivatives of 7-amino-2-(methylthio)[1,2,4]triazolo[1,5-a]pyrimidine-6-carboxylic acid. Synthesis, spectroscopic characterization, in vitro antimicrobial activity and X-ray crystallography

Giuseppe Ruisi [a,*], Loredana Canfora [a], Giuseppe Bruno [b], Archimede Rotondo [b], Teresa F. Mastropietro [c], Eugenio A. Debbia [d], Maria A. Girasolo [a], Bartolomeo Megna [e]

[a] Dipartimento di Chimica Inorganica e Analitica Stanislao Cannizzaro, Università di Palermo, Viale delle Scienze, I-90128 Palermo, Italy
[b] Dipartimento di Chimica Inorganica, Chimica Analitica e Chimica Fisica, Università di Messina, Salita Sperone, 31, I-98166 Messina, Italy
[c] Dipartimento di Chimica, Università della Calabria, I-87030 Arcavacata di Rende, Cosenza, Italy
[d] Sezione di Microbiologia, Di.S.C.A.T., Università di Genova, I-16132 Genova, Italy
[e] Dipartimento di Ingegneria Chimica dei Processi e dei Materiali, Università di Palermo, Viale delle Scienze, I-90128 Palermo, Italy

ARTICLE INFO

Article history:
Received 5 November 2009
Received in revised form 12 November 2009
Accepted 13 November 2009
Available online 20 November 2009

Keywords:
Triazolopyrimidine
Triorganotin(IV) complexes
Crystal structure

ABSTRACT

Triorganotin(IV) complexes of the 7-amino-2-(methylthio)[1,2,4]triazolo[1,5-a]pyrimidine-6-carboxylic acid (HL), $Me_3SnL(H_2O)$, (**1**), $[n\text{-}Bu_3SnL]_2(H_2O)$, (**2**), $Ph_3SnL(MeOH)$, (**3**), were synthesized by reacting the amino acid with organotin(IV) hydroxides or oxides in refluxing methanol. The complexes have been characterized by elemental analysis, ^1H, ^{13}C and ^{119}Sn NMR, IR, Raman and ^{119}Sn Mössbauer spectroscopic techniques. Single crystal X-ray diffraction data were obtained for compounds (**2**) and (**3**). $Ph_3SnL(MeOH)$ presents a trigonal bipyramidal structure with the organic groups on the equatorial plane and the axial positions occupied by a ligand molecule, coordinated to tin through the carboxylate, and a solvent molecule, MeOH. A similar structure is proposed for $Me_3SnL(H_2O)$ on the basis of analytical and spectroscopic data. The tributyltin(IV) derivative, $[n\text{-}Bu_3SnL]_2(H_2O)$, is characterized by two different tin sites with similar tbp geometry featured by butyl groups on the equatorial plane. Sn(1) and Sn(2) atoms are axially bridged by a ligand molecule binding through the N(4) and the carboxylate group; the two coordination spheres are saturated by another ligand molecule, binding the metal through the carboxylate group, and a water molecule, respectively. Antimicrobial tests on compounds **1** and **2** showed in vitro activity against Gram-positive bacteria.

1. Introduction

[1,2,4]Triazolo[1,5-a]pyrimidine derivatives have been extensively used in the synthesis of metal–ion complexes obtaining a variety of new compounds with interesting structural features and relevant biological properties [1,2]. Organotin(IV) complexes were also recently investigated [3,4]. The coordination studies were essentially devoted to alkyl- or oxo-substituted triazolopyrimidines, other substituents being ignored. Carboxylate and amino groups may play an important role in the coordination of organotin(IV) moieties, triorganotin(IV) carboxylates being arousing considerable interest owing to the variety of structures that they may originate [5] and their biological activity [6–13]. Considering the important biological role played by triazolopyrimidines, we decided to investigate the biological and coordinating properties of 7-amino-2-(methylthio)[1,2,4]triazolo[1,5-a]pyrimidine-6-carboxylic acid (HL) complexes with triorganotin(IV) moieties. No literature data were so far reported on this ligand; its structural formula is shown in Fig. 1 with the numbering scheme.

2. Experimental

2.1. Materials

The products employed in the present study were purchased from C. Erba (Milan, Italy), Sigma–Aldrich (Milan, Italy), and Merck (Milan Italy), and used without further purification except methanol, which was distilled over magnesium. The 7-amino-2-(methylthio)[1,2,4]triazolo[1,5-a]pyrimidine-6-carboxylic acid was a May-bridge (UK) product commercialized by C. Erba.

2.2. Physical measurements

Elemental analyses (C, H, N, S) were carried out by the microanalysis laboratory of the Dipartimento di Scienze Chimiche,

* Corresponding author. Fax: +39 091 427584.
E-mail addresses: gruisi@unipa.it (G. Ruisi), loredanacanfora@gmail.com (L. Canfora), gbruno@unime.it (G. Bruno), archi@chem.unime.it (A. Rotondo), teresa.mas@ unical.it (T.F. Mastropietro), eugenio.debbia@unige.it (E.A. Debbia), girasolo@unipa.it (M.A. Girasolo), bartolomegna@gmail.com (B. Megna).

0022-328X/$ - see front matter © 2009 Elsevier B.V. All rights reserved.
doi:10.1016/j.jorganchem.2009.11.019

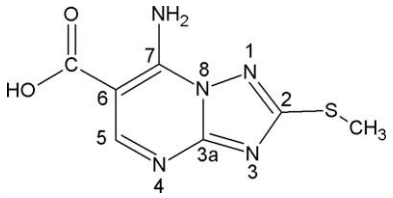

Fig. 1. 7-Amino-2-(methylthio)[1,2,4]triazolo[1,5-a]pyrimidine-6-carboxylic acid (HL).

University of Padua (Italy); tin was gravimetrically determined as SnO_2.

Infrared spectra (nujol and hexachlorobutadiene mulls, CsI windows) were recorded with an FT-IR spectrometer Perkin–Elmer Spectrum ONE in the 4000–250 cm^{-1} region. Raman Spectra were acquired by a MicroRaman, Renishaw InVia Spectrometer, using a 50× magnification lens with a 633 nm laser at an intensity of about 1 mW.

The Mössbauer (nuclear γ resonance) spectrometer, the related instrumentation and data reduction procedures were as previously described [14]. A 10 mCi $Ca^{119}SnO_3$ source (RITVERC GmbH, St. Petersburg, Russia) was employed. The ^1H, ^{13}C and ^{119}Sn NMR spectra were acquired in CD_3OD solutions at 298 K on a Bruker 300 Avance spectrometer at 300.13, 75.47 and 111.92 MHz, respectively.

2.3. Single crystal structural determination by X-ray

Diffraction data for **2** and **3** were measured on a Bruker-Nonius X8 ApexII diffractometer equipped with a CCD area detector by using graphite-monochromated Mo Kα radiation (λ = 0.71073 Å) generated from a sealed tube source. Data were collected and reduced by SMART and SAINT software [15] in the Bruker package. The structure was solved by direct methods [16] and than developed by least squares refinement on F^2 [17]. All non-H atoms were placed in calculated positions and refined as isotropic with the "riding-model technique". Details concerning collection and analysis are reported in Table 1.

The artwork and geometrical parameters are obtained by software programs handled by WINGX software package [18]. The refinement is spoiled by the poor quality of the crystals probably connected with the high thermal motions of the alkyl chains.

2.4. Antimicrobial activity

2.4.1. Bacterial strains

Microorganisms used in this study were isolated from clinical samples. The collection included representative members of the *Enterobacteriaceae* family: *Escherichia coli* (5), *Klebsiella pneumoniae* (5), *Citrobacter freundii* (3), *Morganella morganii* (3), *Enterobacter cloacae* (5), *Proteus mirabilis* (5), as well as *Pseudomonas aeruginosa* (5). Gram-positive strains were *Staphylococcus aureus* (5), *Enterococcus faecalis* (5) and *Streptococcus agalactiae* (2).

2.4.2. Susceptibility tests

The minimum inhibitory concentrations (MIC) of the compounds studied were determined using the microdilution method in Mueller-Hinton broth with the addition of Ca^{2+} and Mg^{2+}. The microplates were incubated aerobically at 35 °C for 18–24 h according to the recommendations of the Clinical and Laboratory Standards Institute [19]. *E. coli* ATCC 25922, *P. aeruginosa* ATCC27853, *S. aureus* ATCC 29213 and *E. faecalis* ATCC 29212 were used as controls.

Table 1
Crystallographic and structure refinement parameters for $[n\text{-}Bu_3SnL]_2(H_2O)$ (**2**) and $Ph_3SnL(MeOH)$ (**3**).

	2	**3**
Empirical formula	$C_{38}H_{68}N_{10}O_5S_2Sn_2$	$C_{26}H_{25}N_5O_3SSn$
Formula weight	1046.58	606.30
Temperature (K)	293(2)	293(2)
Wavelength (Å)	0.71073	0.71073
Crystal system	Orthorhombic	Monoclinic
Space group	*Pbca*	$P2_1/c$
Unit cell dimensions		
a (Å)	23.2329(4)	10.3585(9)
b (Å)	16.2894(3)	26.737(2)
c (Å)	27.6018(5)	9.694(1)
α (°)	90	90
β (°)	90	100.367(2)
γ (°)	90	90
Volume ($Å^3$)	10445.9(3)	2641.0(5)
Z	8	4
Density (calculated) ($g\ cm^3$)	1.331	1.525
Absorption coefficient (mm^{-1})	1.082	1.083
F(0 0 0)	4304	4948
Crystal size (mm^3)	0.3 × 0.26 × 0.08	0.3 × 0.26 × 0.08
θ Range for data collection (°)	4.13–23.60	5.52–25.68
Index ranges	$-26 \leqslant h \leqslant 26$ $-18 \leqslant k \leqslant 18$ $-31 \leqslant l \leqslant 31$	$-12 \leqslant h \leqslant 12$ $-32 \leqslant k \leqslant 32$ $-11 \leqslant l \leqslant 11$
Reflections collected	186489	18960
Independent reflections	7779 [R_{int} = 0.0398]	4948 [R_{int} = 0.0307]
Completeness to θ	0.99	0.99
Absorption correction	None	Sortav
Refinement method	Full-matrix least-squares on F^2	Full-matrix least-squares on F^2
Data/restraints/parameters	7779/229/526	4948/0/326
Goodness-of-fit on F^2	1.064	1.635
Final *R* indices [$I > 2\sigma(I)$]	R_1 = 0.0479, wR_2 = 0.1407	R_1 = 0.0616, wR_2 = 0.1852
R indices (all data)	R_1 = 0.0629, wR_2 = 0.1649	R_1 = 0.0681, wR_2 = 0.1957
Largest difference in peak and hole ($e\ Å^{-3}$)	0.743 and −0.494	3.804 and −0.939

2.4.3. Biofilm production assay

The presence of biofilm was assessed using Congo Red agar plates, as described by Freeman [20].

2.4.4. Evaluation of inhibition of quorum-sensing N-acyl homoserine lactone signal

Chromobacterium violaceum, a generous gift of Robert McLean (Texas State University, San Marcos, USA), was used as biosensor. Quorum sensing inhibition was evaluated either by the overlay procedure described by McLean [21], or by microdilution technique employing *C. violaceum* as test organism.

2.5. Synthesis of the complexes

A suspension of 7-amino-2-(methyltio)[1,2,4]triazolo[1,5-a]pyrimidine-6-carboxylic acid in refluxing methanol was treated with an equimolar amount of triorganotin(IV) hydroxide or oxide. A clear solution was obtained in three or four hours; the solvent was removed *in vacuo* and the residue was repeatedly recrystallized from *n*-hexane/methanol mixtures and finally from methanol giving crystalline solids.

$Me_3SnL(H_2O)$ (**1**) M.p. 259–263 °C dec. *Anal.* Calc. for $C_{10}H_{17}N_5O_3SSn$: C, 29.58; H, 4.22; N, 17.25; S, 7.90; Sn, 29.24. Found: C, 29.72; H, 4.55; N, 17.30; S, 7.75; Sn, 28.50%. IR (cm^{-1}): 1620s $\nu_{asym}(OCO)$, 1361s $\nu_{sym}(OCO)$, 548s $\nu_{asym}(SnC_3)$, 511w $\nu_{sym}(SnC_3)$. Raman (cm^{-1}): 551w $\nu_{asym}(SnC_3)$, 514s $\nu_{sym}(SnC_3)$. ^{119}Sn Mössbauer spectrum: $\delta = 1.26$, $\Delta E = 3.40$, $\Gamma = 0.82$ mm s^{-1}. ^{1}H NMR; δ_H: ligand skeleton: 8.82 [s, 1H, H-5], 2.59 [s, 3H, CH_3–S]; Sn–CH_3: 0.48 [s, 3H, $^2J(^{119}Sn-^1H) = 68.6$ MHz]. ^{13}C NMR; 170.9 [COOH], 169.3 [C-2], 158.0 [C-6], 157.8 [C-5], 150.6 [C-7], 98.5 [C-3a], 13.8 [CH_3–S], −1.6 [CH_3–Sn, $^1J(^{119}Sn-^{13}C) = 512.9$ MHz]. ^{119}Sn NMR; $\delta(^{119}Sn)$: 26.6.

$[n\text{-}Bu_3SnL]_2(H_2O)$ (**2**) M.p. 215–217 °C. *Anal.* Calc. for $C_{38}H_{68}N_{10}O_5S_2Sn_2$: C, 43.61; H, 6.55; N, 13.38; S, 6.13; Sn, 22.68. Found: C, 44.11; H, 6.78; N, 13.30; S, 5.69; Sn, 22.95%. IR (cm^{-1}): 1616s $\nu_{asym}(OCO)$, 1365s $\nu_{sym}(OCO)$, 531m $\nu_{asym}(SnC_2)$. ^{119}Sn Mössbauer spectrum: $\delta = 1.41$, $\Delta E = 3.48$, $\Gamma = 0.76$ mm s^{-1}. ^{1}H NMR; δ_H: ligand skeleton: 8.84 [s, 1H, H-5], 2.70 [s, 3H, CH_3–S]; Sn–nBu_3: 1.73–0.92 [m, 9H]. ^{13}C NMR; 170.8 [COOH], 169.3 [C-2], 158.0 [C-6], 157.7 [C-5], 150.7 [C-7], 98.4 [C-3a], 29.2 [β-CH_2, Bu_3–Sn], 28.1 [γ-CH_2, Bu_3–Sn], 18.7 [α-CH_2, Bu_3–Sn, $^1J(^{119}Sn-^{13}C) = 453.5$ MHz], 14.1 [CH_3, Bu_3–Sn], 13.8 [CH_3–S]. ^{119}Sn NMR; $\delta(^{119}Sn)$: 19.1.

$Ph_3SnL(MeOH)$ (**3**) M.p. 197–199 °C. *Anal.* Calc. for $C_{26}H_{25}N_5O_3SSn$: C, 51.51; H, 4.16; N, 11.55; S, 5.29; Sn, 19.58. Found: C, 51.75; H, 3.99; N, 11.63; S, 5.21; Sn, 19.50%. IR(cm^{-1}): 1605s $\nu_{asym}(OCO)$, 1365s $\nu_{sym}(OCO)$, 272m $\nu_{asym}(SnC_2)$; 574m ν(Sn–O). ^{119}Sn Mössbauer spectrum: $\delta = 1.25$, $\Delta E = 3.12$, $\Gamma = 0.79$ mm s^{-1}. ^{1}H NMR; δ_H: ligand skeleton: 8.80 [s, 1H, H-5], 2.55 [s, 3H, CH_3–S], Sn–Ph_3: 7.80–7.40 [m]. The very low solubility of the triphenyltin derivative did not allow to record ^{13}C and ^{119}Sn NMR spectra for this compound.

3. Results and discussion

3.1. Spectroscopic data

In the infrared spectra of the complexes **1**–**3** the ν(CO) strong band of the ligand (1701 cm^{-1}) is replaced by a couple of intense absorptions in the 1605–1620 and 1361–1365 cm^{-1} regions, which may be attributed to the asymmetric and symmetric $\nu(CO_2)$ stretching mode, respectively. The high values of $\Delta\nu$ (ν_{asym}(O–C=O)−ν_{sym}(O–C=O) > 230 cm^{-1}), strongly suggest an unidentate coordination by the carboxylate group [22].

The arrangement of the carbon atoms in the $Sn(Alk)_3$ group can be easily deduced from the tin–carbon stretching modes which occur in the 550–500 cm^{-1} region of the infrared and Raman spectra [23]. The infrared spectrum of $Me_3SnL(H_2O)$ shows a strong absorption at 548 cm^{-1} and a weak absorption at 511 cm^{-1} which can be assigned to $\nu_{asym}(Sn–C_3)$ and $\nu_{sym}(Sn–C_3)$, respectively. The corresponding absorptions in the Raman spectrum are at 551 and 514 cm^{-1} with reversed intensity. The large difference in the intensity of asymmetric and symmetric $Sn–C_3$ absorptions is indicative of an essentially planar arrangement of the SnC_3 group [23].

The ^{119}Sn Mössbauer spectrum is characterized by a quadruple splitting value of 3.40 mm s^{-1}, fully consistent with a trigonal bipyramidal structure with organic groups in the equatorial plane and electronegative ligands in axial positions [24], tin being 5-coordinate.

The spectral analogies suggest the same ligand arrangement for all triorganotin(IV) complexes in the solid state.

The NMR spectral data point out that the nearly planar arrangement of the organic groups in trialkyltin derivatives is retained in methanol solution. The C–Sn–C bond angle may be evaluated from the coupling constants $|^2J(^{119}Sn-^1H)|$ and $|^1J(^{119}Sn-^{13}C)|$. The relationships derived by Lockhart and Manders for methyltin(IV) derivatives give C–Sn–C bond angles of 119° ($|^2J|$, Ref. [25]) and 121° ($|^1J|$, Ref. [26]), for compound (**1**) while the relationship proposed by Holeček and Lička for *n*-butyltin(IV) derivatives give a C–Sn–C bond angle of 120° ($|^1J|$, Ref. [27]) for compound (**2**). Besides, the values of $\delta(^{119}Sn)$ are compatible with five-coordinate trialkyltin(IV) compounds [28].

In the solid state, tin expands his coordination number through bridge coordination of the ligand or the coordination of a solvent molecule. The ligand would in principle bind tin atom through the amino group, an endocyclic nitrogen atom or the thioether sulphur atom. The latter possibility is excluded by the absence of stretching absorptions which may be assigned to Sn–S bonds [29]. Concerning the amino group, the infrared spectra of the complexes do not show meaningful changes in the N–H stretching frequencies, as expected on the basis of the low basicity of the amine nitrogen, due to the electron-drawing effect of the carboxylic group and the endocyclic nitrogen N(4). N(4) and N(3) are then the most probable coordination sites, according to the structures reported for metal derivatives of triazolopyrimidines [1].

The presence of a N(3)–Sn or N(4)–Sn bond is hard to diagnose as the ν(Sn–N) stretching frequencies have been reported on an extremely wide range, so, considering the high number of the ligand absorptions, it is not possible to make unambiguous assignments. The N(3)–metal bond causes a shift of the ν(tp) and ν(py) frequencies assigned to the vibrations of triazolopyrimidine and pyrimidine ring, respectively. Such shifts, however, have been observed only in the spectra of the triazolopyrimidine (tp) and its derivatives containing alkyl or aryl groups in 5 and 7 positions, which coordinate the metal centre only through N(3) [4]. On the other hand, the coordination of metallic ions through N(3) do not influences ^{1}H and ^{13}C NMR spectra nearly at all, as observed in stable metal complexes of 5,7-dimethyltriazolopyrimidine [30]. Also the ^{15}N NMR spectra are very little influenced by coordination, shifts of about 0.5 ppm having been observed in spectra of Zn(II) complexes of tp, dmtp, dptp and dbtp, in contrast with the 10–60 ppm shifts observed in other complexes with N-donor molecules, such as imidazole or 1-methylimidazole [31].

The spectroscopic data suggest a tbp structure for triorganotin(IV) derivatives where C atoms of the organotin moiety lie on the equatorial plane while the axial positions are occupied by an unidentate carboxylate group and an endocyclic nitrogen atom. X-ray crystallographic data are consistent with the spectroscopic evidences, but they show slight differences in the molecular structures of the tri-*n*-butyltin(IV) **2** and triphenyltin(IV) **3** complexes

with the 7-amino-2-(methylthio)[1,2,4]triazolo[1,5-a]pyrimidine-6-carboxylic acid, pointing out that water and methanol molecules coordinate tin.

3.2. X-ray crystallography

Colourless crystals, suitable for the X-ray analysis, where obtained by slow evaporation from methanol solutions. X-ray reflections analysis shows that **2** crystallizes in the orthorhombic space group *Pbca*. The asymmetric unit is occupied by a neutral bimetallic complex with two non-equivalent Sn atoms. Beyond the expected alkyl groups, two ligands L and a water molecule populate the metals' coordination spheres (Fig. 2).

Both metallic centres keep the tbp coordinating geometry often shown by trialkyl-tin with oxygenated and nitrogenated axial ligands (Table 2) [32]. The two L ligands result different since one coordinates Sn1 just by the O15 of the carboxylate group, whereas the other one bridges the two metals binding Sn1 through the N32 of the purine moiety and Sn2 with O42 on the carboxylate group.

The position of the axial binding atoms is remarkably asymmetrical because of the negative electron density over the carboxylate O atoms which thus approach the metal more than the opposing axial atom (Table 2 and similar structures [33]). The long Sn1–N32 distance (2.620(3) Å) is not really unexpected since other similar systems show this same feature [33b]. The whole three-dimensional structure is supported by hydrogen interactions occurring between the several H-donors and acceptors (Fig. 3, Table 3). It has to be mentioned also a staggered graphitic interaction between the aromatic cores of two L units belonging to molecules related by the symmetry operation $-x$, $-y$, $-z+1$ (distance between mean planes 3.352(3) Å), whose edges (N3–C4–N5) are closer than the sum of atoms van der Waals radii.

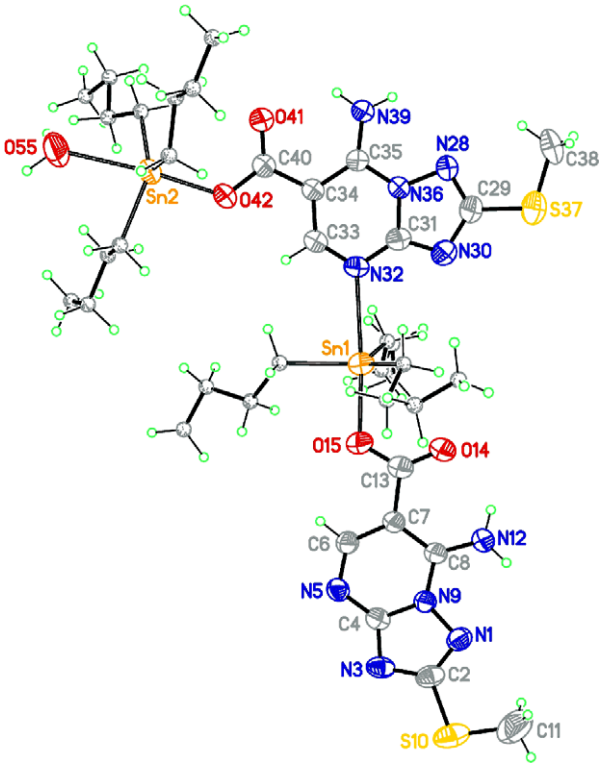

Fig. 2. ORTEP molecular representation for **2** with atom labelling scheme. Ellipsoids of 30% probability are shown for anisotropic atoms, while *n*-butyl groups, thermally disordered, and hydrogen atoms are depicted as arbitrary radium spheres.

Table 2
Selected bond distances (Å) and angles (°) for **2** and **3**.

Structure **2**		Structure **3**	
Sn1–C16	2.115(6)	Sn1–C16	2.123(5)
Sn1–C20	2.153(6)	Sn1–C22	2.146(5)
Sn1–C24	2.118(6)	Sn1–C28	2.127(5)
Sn1–O15	2.157(3)	Sn1–O15	2.142(4)
Sn1–N32	2.620(3)	Sn1–O34	2.507(4)
Sn2–C43	2.131(5)		
Sn2–C47	2.131(5)		
Sn2–C51	2.130(4)		
Sn2–O42	2.133(3)		
Sn2–O55	2.573(4)		
C20–Sn1–C16	112.8(3)	C16–Sn1–C22	111.5(2)
C24–Sn1–C20	126.4(2)	C16–Sn1–C28	125.1(2)
C24–Sn1–C16	115.5(7)	C22–Sn1–C28	111.5(2)
O15–Sn1–C16	89.3(2)	O15–Sn1–C16	96.8(2)
O15–Sn1–C20	96.8(2)	O15–Sn1–C22	90.8(2)
O15–Sn1–C24	98.7(2)	O15–Sn1–C28	100.9(2)
O15–Sn1–N32	176.0(1)	O15–Sn1–O34	176.7(1)
C24–Sn1–N32	83.6(2)	C16–Sn1–O34	83.3(2)
C20–Sn1–N32	84.4(2)	C22–Sn1–O34	86.2(2)
C16–Sn1–N32	86.7(2)	C28–Sn1–O34	81.6(2)
C43–Sn2–C47	121.4(2)		
C43–Sn2–C51	117.8(2)		
C47–Sn2–C51	118.6(2)		
O55–Sn2–C43	86.5(2)		
O42–Sn2–C43	97.8(2)		
O42–Sn2–C47	96.8(2)		
O42–Sn2–C51	90.4(2)		
O55–Sn2–C47	82.7(2)		
O55–Sn2–C51	85.7(1)		
O55–Sn2–O42	175.2(1)		

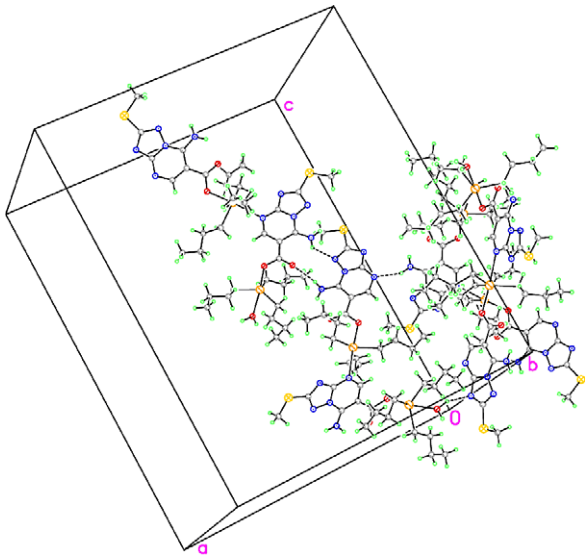

Fig. 3. The XP(Bruker) packing diagram of a unit cell of **2**. The most relevant hydrogen interactions are evidenced as dashed lines.

Table 3
Hydrogen interactions with related structural parameters for **2** (Å and °).

D–H···A	(D–H) (Å)	(H···A) (Å)	(D···A) (Å)	(D–H···A) (°)
N12–H12A···O41$^{\#1}$	0.86	2.19	2.920(7)	142.2
N12–H12B···O14	0.86	2.06	2.674(7)	127.3
N39–H39A···N5$^{\#2}$	0.86	2.14	2.924(6)	152.1
N39–H39B···O41	0.86	2.11	2.714(6)	126.4
N39–H39B···N1$^{\#3}$	0.86	2.54	3.183(6)	132.6
O55–H55B···N3$^{\#4}$	0.94	2.11	2.781(7)	126.8

Symmetry transformations used to generate equivalent atoms: #1 $-x+1/2$, $-y$, $z+½$; #2 $x+1/2$, y, $-z+½$; #3 $-x+1/2$, $-y$, $z-½$; #4 $-x$, $y+1/2$, $-z+1/2$.

Compound **3** crystallizes in the monoclinic $P2_1/c$ space group, shows a tbp monometallic complex whose axial Sn1 binding atoms are the carboxylate O15 coming from an L unit, and the O34 belonging to a coordinated methanol molecule (Fig. 4). Beyond the peripheral molecular differences, the Sn coordination geometries for structures **2** and **3** present similar features as shown in Table 2. The main intermolecular hydrogen interaction for the solid state of **3** generates a one-dimensional array of molecules along the diagonal of the *a* and *c* crystallographic axes (Table 4 and Fig. 5). Other weaker dipolar interactions support the molecular packing along the other directions.

3.3. Antimicrobial activity

Owing to the low solubility of the triphenyltin compound and of the ligand itself, antimicrobial activity tests were effected only on compounds **1** and **2**. The great majority of Gram-negative tested organisms (31) resulted poorly susceptible to compound **2**, the MIC values ranging from 1000 to 2000 mg/L, while Gram-positive isolates (12) were all inhibited at a dose ⩽4 mg/L of the compound with the exception of the two strains of *S. agalactiae* which exhibited MIC values of 0.5 and 2 mg/L (data not shown). The in vitro activity of **1** was similar to that of **2**, against many members of the *Enterobacteriaceae* family (MIC ⩾ 1000 mg/L). Some differences were found in the MIC values registered with *P. aeruginosa* (MIC = 250 mg/L) and in a single isolate of *E. coli*, *E. cloacae* and *P. mirabilis* (MIC = 500 mg/L). Gram-positive bacteria resulted inhibited at concentrations ⩾1000 mg/L with the exception of *S. agalactiae* (MIC = 32 mg/L).

As reported in Table 5 both compounds **1** and **2** at a sub-MIC concentration (500 mg/L) inhibited biofilm production in all the Gram-negative bacteria studied, swarming in *P. mirabilis*, and pigment production in *P. aeruginosa*. Similar results were obtained employing the comparative agent azithromycin. With respect to Gram-positive isolates, biofilm-inhibition was not found exposing the bacteria to sub-inhibitory concentration of compound **2**, while both azithromycin and **1** affected this trait in all the strains tested. When *C. violaceum* was used as biosensor for quorum-sensing

Table 4
Hydrogen interactions with related structural parameters for **3** (Å and °).

D–H···A	(D–H) (Å)	(H···A) (Å)	(D···A) (Å)	(D–H···A) (°)
O34–H34···N3$^{\#1}$	0.96	1.95	2.842(6)	153.7
N12–H12B···O14	0.86	2.05	2.665(6)	127.8

Symmetry transformations used to generate equivalent atoms: #1 $x-1, y, z-1$.

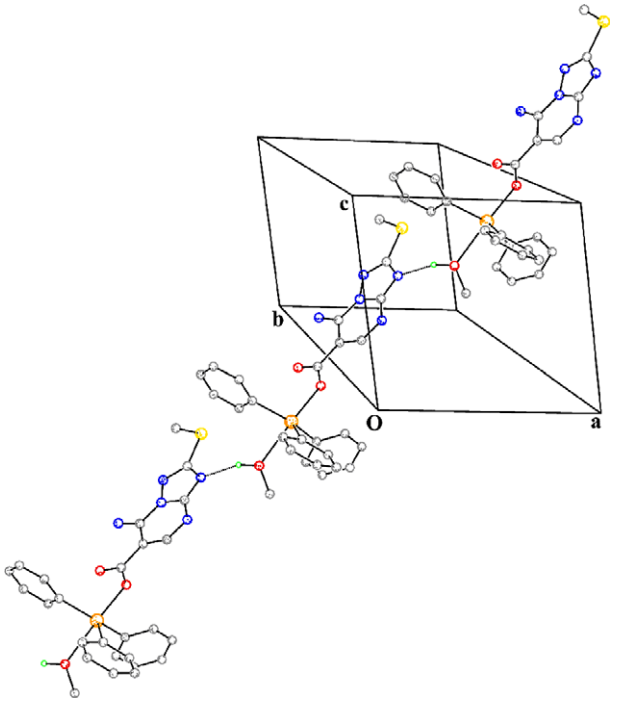

Fig. 5. 1D molecular array of **3** (in balls and sticks) along the [1 0 1] crystallographic direction. Intermolecular hydrogen bonds are represented as dashed lines. Hydrogens not involved in the intermolecular interaction are omitted for clarity.

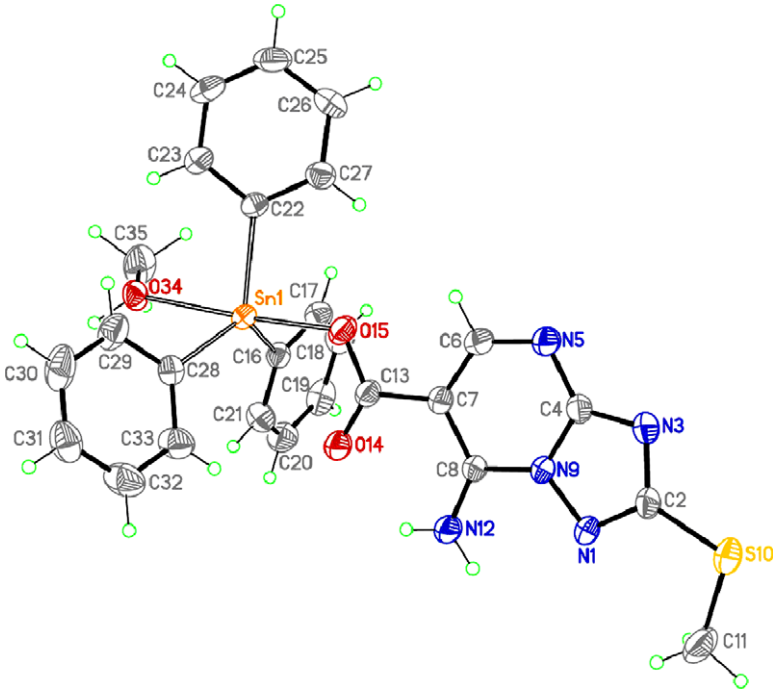

Fig. 4. ORTEP representation of **3** with atom labelling scheme. Thermal ellipsoids are drawn at the 30% probability level.

Table 5
Effects of compounds **1** and **2** (0.5 × MIC) and azithromycin, as comparative agent, on pathogenicity traits of representative biofilm-producing microorganisms.

	Compound **1** Pathogenicity trait			Compound **2** Pathogenicity trait			Azithromycin Pathogenicity trait		
Strains (no. of strains tested)	Biofilm	Pigment	Swarming	Biofilm	Pigment	Swarming	Biofilm	Pigment	Swarming
E. coli (5)	+	na	na	+	na	na	+	na	na
K. pneumoniae (3)	+	na	na	+	na	na	+	na	na
E. cloacae (2)	+	na	na	+	na	na	+	na	na
C. freundii (1)	+	na	na	+	na	na	+	na	na
M. morganii (1)	+	na	na	+	na	na	+	na	na
P. mirabilis (3)	+	na	+	+	na	+	+	na	+
P. aeruginosa (5)	+	+	na	+	+	na	nt	+	na
S. aureus (3)	+	na	na	–	na	na	+	na	na
E. faecalis (3)	+	na	na	–	na	na	+	na	na
E. coli ATCC 25922	na	na	na	np	na	na	na	na	na
P. aeruginosa ATCC 27853	nt	+	na	np	+	na	nt	+	na
S. aureus ATCC 29213	+	na	na	–	na	na	+	na	na
E. faecalis ATCC 29212	+	na	na	–	na	na	+	na	na
C. violaceum ATCC 12477	nt	+	na	nt	+	na	nt	+	na

+ or –: inhibition or not inhibition of the trait tested on all strains, respectively, na: not applicable, nt: not tested, np: non-producing.

signals, it demonstrated susceptibility to compound **2** (MIC = 4 mg/L, the same value registered with azithromycin) and **1** (MIC = 32 mg/L). In the tests for the evaluation of pigment production all the compounds demonstrated to affect violacein synthesis under the same experimental conditions (0.5 × MIC).

The present findings indicate that the in vitro activity of these compounds against both Gram-positive and Gram-negative bacteria varied in an unpredictable way. This is probably due to the different ability of the compounds to cross the cell wall of Gram-positives and Gram-negative bacteria. An interesting point is the inhibition of the quorum-sensing signal in all the species. Although it was noted in some circumstances at high concentration (500 mg/L), it demonstrated a specific influence of this phenomenon in all the strains studied. Since quorum-sensing in Gram-positive and Gram-negative isolates is mediated by different compounds [34], both compounds **1** and **2** appeared to affect acyl-homoserine lactone family compounds while **1** resulted to possess activity also on Gram-positive mediators as seen in biofilm production of Gram-positive strains. Although this last point requires further studies, these compounds appear good candidates to circumvent antibiotic resistance problem interfering with virulence and pathogenicity traits in bacteria, that is considered the new strategy for the therapy of infectious diseases.

Acknowledgements

The financial support of the Università di Palermo, Italy, is gratefully acknowledged.

Appendix A. Supplementary material

CCDC 735808 and 735809 contain the supplementary crystallographic data for **2** and **3**. These data can be obtained free of charge from The Cambridge Crystallographic Data Centre via www.ccdc.cam.ac.uk/data_request/cif. Supplementary data associated with this article can be found, in the online version, at doi:10.1016/j.jorganchem.2009.11.019.

References

[1] J.M. Salas, M.A. Romero, M.P. Sánchez, M. Quirós, Coord. Chem. Rev. 193–195 (1999) 1119.
[2] J.G. Haasnot, Coord. Chem. Rev. 200–202 (2000) 131.
[3] M.A. Girasolo, C. Di Salvo, D. Schillaci, G. Barone, A. Silvestri, G. Ruisi, J. Organomet. Chem. 690 (2005) 4773.
[4] M.A. Girasolo, D. Schillaci, C. Di Salvo, G. Barone, A. Silvestri, G. Ruisi, J. Organomet. Chem. 691 (2006) 693.
[5] V. Chandrasekhar, S. Nagendran, V. Baskar, Coord. Chem. Rev. 235 (2002) 1.
[6] L. Pellerito, L. Nagy, Coord. Chem. Rev. 224 (2002) 111.
[7] H.I. Beltrán, R. Santillan, N. Farfán, Biological aspects of organotins perspectives in structural and molecular biology, in: M. Gielen, A.G. Davies, K.H. Tiekink, E.R.T. Pannell (Eds.), Tin Chemistry Fundamentals, Frontiers, and Applications, John Wiley & Sons, Ltd., Chichester, UK, 2008, p. 482.
[8] M. Ashfaq, J. Organomet. Chem. 691 (2006) 1803.
[9] M. Gielen, M. Biesemans, R. Willem, Appl. Organomet. Chem. 19 (2005) 440.
[10] M. Gielen, Appl. Organomet. Chem. 16 (2002) 481.
[11] X. Shang, J. Cui, J. Wu, A.J.L. Pombeiro, Q. Li, J. Inorg. Biochem. 102 (2008) 901.
[12] Q. Li, M.F.C. Guedes da Silva, A.J.L. Pombeiro, Chem. Eur. J. 10 (2004) 1456.
[13] X. Shang, J. Wu, A.J.L. Pombeiro, Q. Li, Appl. Organomet. Chem. 21 (2007) 919.
[14] R. Barbieri, G. Ruisi, A. Silvestri, A.M. Giuliani, A. Barbieri, G. Spina, F. Pieralli, F. Del Giallo, J. Chem. Soc., Dalton Trans. (1995) 467. and references therein.
[15] Bruker AXS Inc., SMART (Version 5.060) and SAINT (Version 6.02), Madison, Wisconsin, USA, 1999.
[16] M.C. Burla, R. Caliandro, M. Camalli, B. Carrozzini, G.L. Cascarano, L. De Caro, C. Giacovazzo, G. Polidori, R. Spagna, J. Appl. Cryst. 38 (2005) 381.
[17] (a) G.M. Sheldrick, SHELXL97, Program for Crystal Structure Refinement, University of Göttingen, Germany, 1997.;
(b) SHELXTL NT, Version 5.10, Bruker Analytical X-ray Inc., Madison, WI, USA, 1998.
[18] L.J. Farrugia, Appl. Crystallogr. 32 (1999) 837.
[19] Clinical and Laboratory Standards Institute. Performance standards for antimicrobial susceptibility testing, 19th informational supplement, document M100-S19, Wayne, PA, USA, CLSI 2009.
[20] D.J. Freeman, F.R. Falkiner, C.T. Keane, J. Clin. Pathol. 42 (1989) 872.
[21] R.J.C. McLean, L.S. Pierson III, C.J. Fuqua, Microbiol. Methods 58 (2004) 351.
[22] G.B. Deacon, F. Huber, R.J. Phillips, Inorg. Chim. Acta 104 (1985) 41.
[23] B.Y.K. Ho, J.J. Zuckerman, Inorg. Chem. 12 (1973) 1552.
[24] R. Barbieri, F. Huber, L. Pellerito, G. Ruisi, A. Silvestri, Tin-119m Mössbauer Studies on Tin Compounds, in: P.J. Smith (Ed.), Chemistry of Tin, Chapman and Hall, London, 1998, p. 496 (Chapter 14).
[25] T.P. Lockhart, W.F. Manders, Inorg. Chem. 25 (1986) 892.
[26] T.P. Lockhart, W.F. Manders, J. Am. Chem. Soc. 109 (1987) 7015.
[27] J. Holeček, A. Lyčka, Inorg. Chim. Acta 118 (1986) L15.
[28] M. Návdorník, J. Holeček, K. Handlíř, A. Lyčka, J. Organomet. Chem. 275 (1984) 43.
[29] N. Ohkaku, K. Nakamoto, Inorg. Chem. 12 (1973) 2449.
[30] E. Szłyk, A. Grodzicki, L. Pazderski, J. Sitkowski, Polish J. Chem. 72 (1998) 55.
[31] E. Szłyk, A. Grodzicki, L. Pazderski, E. Bednarek, B. Kamieński, Polyhedron 19 (2000) 965.
[32] S. Bhandari, C.G. Frost, C.E. Hague, M.F. Mahon, K.C. Molloy, J. Chem. Soc., Dalton Trans. (2000) 663.
[33] (a) K.M. Lo, S.W. Ng, Main Group Met. Chem. 23 (2000) 733;
(b) S.W. Ng, Z. Kristallogr.- New Cryst. Struct. 213 (1998) 157;
(c) H.D. Yin, S.W. Chen, Inorg. Chim. Acta 359 (2006) 3330;
(d) S.G. Teoh, D.S. Tan, G.-Y. Yeap, H.-K. Fun, Z. Kristallogr.- New Cryst. Struct. 214 (1999) 161;
(e) K.M. Lo, S.W. Ng, V.G. Kumar Das, Acta Crystallogr., Sect. C 53 (1997) 545.
[34] B.L. Bassler, R. Losick, Cell 125 (2006) 237.